J|A|C|S
COMMUNICATIONS

Published on Web 12/31/2005

Magnetic Fluorescent Delivery Vehicle Using Uniform Mesoporous Silica Spheres Embedded with Monodisperse Magnetic and Semiconductor Nanocrystals

Jaeyun Kim,[†] Ji Eun Lee,[†] Jinwoo Lee,[†] Jung Ho Yu,[†] Byoung Chan Kim,[‡] Kwangjin An,[†] Yosun Hwang,[§] Chae-Ho Shin,[¶] Je-Geun Park,[§] Jungbae Kim,[‡] and Taeghwan Hyeon*[,†]

Center for Oxide Nanocrystalline Materials and School of Chemical and Biological Engineering, Seoul National University, Seoul 151-744, Korea, Pacific Northwest National Laboratory, Richland, Washington 99352, Department of Physics and Institute of Basic Science, Sungkyunkwan University, Suwon 440-746, Korea, and Department of Chemical Engineering, Chungbuk National University, Cheongju 360-763, Korea

Received September 26, 2005; E-mail: thyeon@plaza.snu.ac.kr

Uniform-sized colloidal nanocrystals have attracted much attention because of their unique magnetic and optical properties, as compared with those of their bulk counterparts.[1] Especially, magnetic nanocrystals and quantum dots have been intensively pursued for biomedical applications, such as contrast enhancement agents in magnetic resonance imaging, magnetic carriers for drug delivery systems, biological labeling, and diagnostics.[2] Due to their large pore size and high surface area, mesoporous materials and their composites with nanocrystals have attracted considerable attention.[3] To use nanocrystals as functional delivery carriers and catalytic supports, nanocrystals coated with porous silica shells are desirable. There have been a few reports on the preparation of nanocrystals coated with mesoporous shells. Gold nanoparticles stabilized with mercaptopropyltrimethoxysilane were coated with mesoporous silica shells via sol−gel reaction on the surface of the nanoparticles.[4] Nanorattles composed of gold nanoparticles encapsulated in mesoporous carbon and polymer shells were synthesized.[5] Pt nanoparticles stabilized with poly(vinylpyrrolidone) were coated with mesoporous silica shells through sol−gel reaction.[6] Magnetic core/mesoporous silica shell structures were synthesized by sol−gel reaction on hematite particles followed by H_2 reduction.[7] Herein, we report a synthetic procedure for the fabrication of monodisperse nanocrystals embedded in uniform pore-sized mesoporous silica spheres. As a representative example, we synthesized monodisperse magnetite (Fe_3O_4) nanocrystals embedded in mesoporous silica spheres and both magnetite nanocrystals and CdSe/ZnS quantum dots embedded in mesoporous silica spheres. Furthermore, these mesoporous silica spheres were applied to the uptake and controlled release of drugs.

A typical procedure for the synthesis of the magnetite nanocrystal embedded in mesoporous silica spheres (M-MSS) is shown in Scheme 1.[8] As-prepared 12 nm sized magnetite nanocrystals are typically stabilized with hydrophobic oleic acid ligands and are dispersed in nonpolar organic solvents. To conduct sol−gel reaction to form mesoporous silica spheres, it was necessary to transfer these hydrophobic ligand-capped nanocrystals from organic phase to aqueous phase. Recently, Fan et al. reported water-dispersible gold nanocrystals prepared using various surfactants.[9] We used a similar approach to prepare water-dispersible nanocrystals, employing cetyltrimethylammonium bromide (CTAB) as a secondary surfactant. The subsequent sol−gel reaction of tetraethyl orthosilicate (TEOS) in an aqueous solution containing CTAB (and oleic acid)-stabilized magnetite nanocrystals and small amount of ethyl acetate

Scheme 1. Synthetic Procedure of Monodisperse Magnetite Nanocrystals Embedded in Mesoporous Silica Spheres (M-MSS)

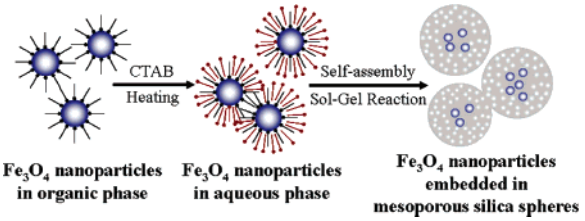

followed by removal of the organic templates generated M-MSS. CTAB-stabilized nanocrystals acted as seeds for the formation of spherical mesoporous silica particles. CTAB served as not only the stabilizing secondary surfactant for the transfer of the nanocrystals to the aqueous phase but also the organic template for the formation of the mesoporous silica spheres. Magnetite nanocrystals and green-emitting CdSe/ZnS quantum dots were simultaneously embedded in mesoporous silica spheres (M/GQD-MSS).

FE-SEM image (Figure 1a) and TEM images (Figure 1b,c) of M-MSS revealed that the mesoporous silica spheres are quite uniform in size with an average particle diameter of around 150 nm, which is within applicable size range for drug and gene delivery.[10] Each silica sphere contained several monodisperse magnetite nanocrystals. The hollow-like core structure seemed to result from the trapping of ethyl acetate in the hydrophobic part during sol−gel reaction.[8] HRTEM image (Figure 1d) indicated that the silica spheres possessed disordered mesopores (~4 nm) derived from CTAB-templating, and that the embedded magnetite nanocrystals retained the original crystallinity. M/GQD-MSS had uniform spherical morphology (Figure 1e) similar to that of M-MSS

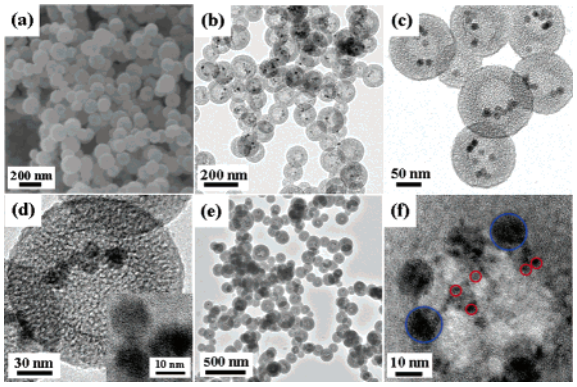

Figure 1. FE-SEM (a), TEM (b, c), and HRTEM (d) images of M-MSS and TEM (e), and HRTEM (f) images of M/GQD-MSS (blue circles for magnetite nanocrystals and red circles for quantum dots).

[†] Seoul National University.
[‡] Pacific Northwest National Laboratory.
[§] Sungkyunkwan University.
[¶] Chungbuk National University.

10.1021/ja0565875 CCC: $33.50

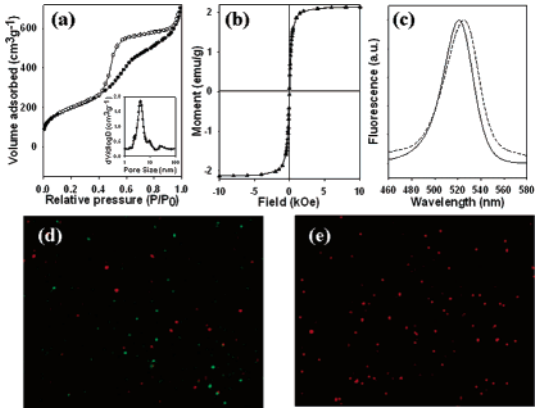

Figure 2. N_2 adsorption/desorption isotherms (inset: PSD from adsorption branch) (a) and field-dependent magnetization at 300 K (b) of M-MSS, PL spectra ($\lambda_{ex} = 450$ nm) of pristine CdSe/ZnS nanoparticles (solid line) and M/GQD-MSS (dotted line) (c), and confocal microscope images from a mixture suspension of RQD-MSS and M/GQD-MSS before (d) and after (e) removal of M/GQD-MSS by magnetic separation.

and encapsulated both magnetite nanocrystal and CdSe/ZnS quantum dots (Figure 1f).

The N_2 adsorption/desorption isotherms (Figure 2a) exhibited a type IV isotherm with a hysteresis loop, demonstrating their mesoporous characteristics. The pore size calculated using the BJH method (Figure 2a, inset) was 3.5 nm. The uniform mesopores along with small particle size (<200 nm) are advantageous for the drug delivery applications compared to commercially available micrometer-sized magnetic polymeric beads. The BET surface area and the total pore volume were 721 $m^2\ g^{-1}$ and 1.09 $cm^3\ g^{-1}$, respectively. Field-dependent magnetism at 300 K showed no hysteresis (Figure 2b), which represented that M-MSS, obtained after removal of organic templates, exhibited the superparamagnetic characteristics desirable for their applications to delivery and separation. The bare 3.5 nm sized CdSe/ZnS quantum dots and the resulting M/GQD-MSS exhibited emission peaks at a similar position with a slight red-shift (Figure 2c). To demonstrate the importance of magnetic separation (guiding), the combined magnetic and luminescent properties of M/GQD-MSS were tested simultaneously. We prepared 6 nm sized red-emitting CdSe/ZnS nanocrystals and subsequently embedded them in mesoporous silica spheres (RQD-MSS). Then, RQD-MSS and M/GQD-MSS were mixed in water, and magnetic separation was performed. The confocal microscope image of the mixed solution (Figure 2d) showed that red and green dots coexisted, whereas only red dots remained after magnetic separation of M/GQD-MSS using a magnet (Figure 2e), demonstrating that green-emitting M/GQD-MSS was completely separated from the mixture by a magnet.

To investigate M-MSS as a candidate of drug carriers for delivery, we selected ibuprofen as a model drug, which is well-known as a nonsteroidal anti-inflammatory agent and contains a carboxyl group in the molecular structure. An additional sample was prepared by further functionalizing M-MSS with 3-(aminopropyl)triethoxysilane, denoted as M-MSS−NH_2. We adsorbed ibuprofen into MSS's with different surface properties: M-MSS with silanol groups and M-MSS−NH_2 with amino groups. The loadings of ibuprofen in M-MSS and M-MSS−NH_2 were 18 and 13 wt %, respectively. The decrease of ibuprofen loading in M-MSS−NH_2 can be ascribed to the reduction of surface area from 706 to 302 m^2/g by the surface modification. However, when the ibuprofen loadings are normalized by the surface area, M-MSS−NH_2 resulted in a higher loading than M-MSS.[8] This suggests that favorable interaction between the amino group on M-MSS−NH_2 and the carboxyl group of ibuprofen increased the ibuprofen loading

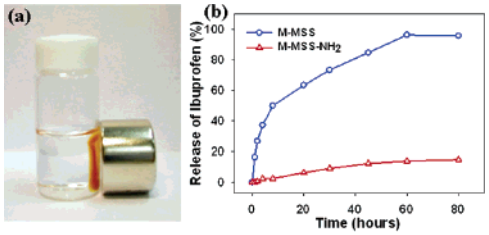

Figure 3. (a) A photograph showing magnetic capture of M-MSS. (b) Release of ibuprofen from M-MSS and M-MSS−NH_2.

per surface area in M-MSS−NH_2. To measure the amount of released ibuprofen, the mesoporous silica spheres in buffer solution were captured by using a magnet (Figure 3a). Figure 3b shows the release of ibuprofen from M-MSS and M-MSS−NH_2; 95% of the adsorbed ibuprofen was release from M-MSS within 60 h, while M-MSS−NH_2 could delay the release of ibuprofen in a vivid fashion. For example, only 15% of adsorbed ibuprofen was released from M-MSS−NH_2 even after 80 h incubation, suggesting that the favorable ionic interaction between the amino group on M-MSS−NH_2 and the carboxyl group of ibuprofen prevents the easy release of ibuprofen. This demonstrated that the release rate of a drug from M-MSS can be controlled by the surface modification of the silica spheres.

In conclusion, we synthesized monodisperse magnetite nanocrystals and quantum dots embedded in uniform pore-sized mesoporous silica spheres with an average particle size of 150 nm. Mesoporous silica spheres adsorbed ibuprofen, and the release rate of ibuprofen was controlled by the surface properties of mesoporous silica spheres. These mesoporous silica spheres are likely to find many biomedical applications.

Acknowledgment. We thank the National Creative Research Initiative Program of the Korean Ministry of Science and Technology for the financial support.

Supporting Information Available: The Experimental Section, TEM images, mechanism, and ibuprofen loadings. This material is available free of charge via the Internet at http://pubs.acs.org.

References

(1) Schmid, G. *Nanoparticles: From Theory to Application*; Wiley-VCH: Weinheim, Germany, 2004.
(2) (a) Murray, C. B.; Norris, D. J.; Bawendi, M. G. *J. Am. Chem. Soc.* **1993**, *115*, 8706−8715. (b) Sun, S.; Murray, C. B.; Weller, D.; Folks, L.; Moser, A. *Science* **2000**, *287*, 1989−1992. (c) Hyeon, T. *Chem. Commun.* **2003**, 927−934.
(3) (a) Kresege, C. T.; Leonowicz, M. E.; Roth, W. J.; Vartuli, J. C.; Beck, J. S. *Nature* **1992**, *359*, 710−712. (b) Zhao, D.; Feng, J.; Huo, Q.; Melosh, N.; Fredrickson, G. H.; Chmelka, B. F.; Stucky, G. D. *Science* **1998**, *279*, 548−552. (c) Ying, J. Y.; Mehnert, C. P.; Wong, M. S. *Angew. Chem., Int. Ed.* **1999**, *38*, 56−77. (d) Garcia, C. B. W.; Zhang, Y.; Mahajan, S.; DiSalvo, F.; Wiesner, U. *J. Am. Chem. Soc.* **2003**, *125*, 13310−13311. (e) Wong, M. S.; Cha, J. N.; Choi, K.-S.; Deming, T. J.; Stucky, G. D. *Nano Lett.* **2002**, *2*, 583−587.
(4) Nooney, R. I.; Dhanasekaran, T.; Chen, Y.; Josephs, R.; Ostafin, A. E. *Adv. Mater.* **2002**, *14*, 529−532.
(5) Kim, M.; Sohn, K.; Na, H. B.; Hyeon, T. *Nano Lett.* **2002**, *2*, 1383−1387.
(6) Lin, K.-J.; Chen, L.-J.; Prasad, M. R.; Cheng, C.-Y. *Adv. Mater.* **2004**, *16*, 1845−1849.
(7) Zhao, W.; Gu, J.; Zhang, L.; Chen, H.; Shi, J. *J. Am. Chem. Soc.* **2005**, *127*, 8916−8917.
(8) For details, see Supporting Information.
(9) (a) Fan, H.; Yang, K.; Boye, D. M.; Sigmon, T.; Malloy, K. J.; Xu, H.; Lüpez, G. P.; Brinker, C. J. *Science* **2004**, *304*, 567−571. (b) Fan, H.; Leve, E. W.; Scullin, C.; Gabaldon, J.; Tallant, D.; Bunge, S.; Boyle, T.; Wilson, M. C.; Brinker, C. J. *Nano Lett.* **2005**, *5*, 645−648. (c) Fan, H.; Chen, Z.; Brinker, C. J.; Clawson, J.; Alam, T. *J. Am. Chem. Soc.* **2005**, *127*, 13746−13747.
(10) (a) Lai, C.-Y.; Trewyn, B. G.; Jeftinija, D. M.; Jeftinija, K.; Xu, S.; Jeftinija, S.; Lin, V. S.-Y. *J. Am. Chem. Soc.* **2003**, *125*, 4451−4459. (b) Radu, D. R.; Lai, C.-Y.; Jeftinija, K.; Rowe, E. W.; Jeftinija, S.; Lin, V. S.-Y. *J. Am. Chem. Soc.* **2004**, *126*, 13216−13217.

JA0565875